CO2 Uptake Potential of Ca-Based Air Pollution Control Residues over Repeated Carbonation–Calcination Cycles

Author(s):
Dal Pozzo, Alessandro; Armutlulu, Andac; Rekhtina, Margarita; Müller, Christoph R.; Cozzani, Valerio

Publication date:
2018-04-19

Permanent link:
https://doi.org/10.3929/ethz-b-000258107

Originally published in:
Energy & Fuels 32(4), https://doi.org/10.1021/acs.energyfuels.8b00391

CO_2 Uptake Potential of Ca-based Air Pollution Control (APC) Residues over Repeated Carbonation/Calcination Cycles

Alessandro Dal Pozzo [a], Andaç Armutlulu [b], Margarita Rekhtina [b], Christoph R. Müller [b], Valerio Cozzani [a,]*

[a] Laboratory of Industrial Safety and Environmental Sustainability, Department of Civil, Chemical, Environmental and Materials Engineering, Alma Mater Studiorum - Università di Bologna, via Terracini 28, 40131 Bologna, Italy

[b] Laboratory of Energy Science and Engineering, Department of Mechanical and Process Engineering, ETH Zürich, Leonhardstrasse 21, 8092 Zürich, Switzerland

Keywords. CO_2 capture; Calcium looping; Waste-to-energy; APC residues; Calcium-based sorbents.

ABSTRACT. Operation of dry processes for acid gas removal from flue gas in waste-to-energy plants based on the use of calcium hydroxide as a solid sorbent generates a solid waste stream containing fly ash, unreacted calcium hydroxide and the products of its reaction with acid pollutants in the flue gas (HCl and SO_2). To date, the fate of the solid waste stream is to be

landfilled, in the absence of commercially viable recycling approaches. The present study investigates the potential of these residues as CO_2 sorbents in the calcium looping process. Samples collected in different waste-to-energy plants were tested over multiple carbonation/calcination cycles, comparing their performance to that of limestone. Though inferior, the CO_2 sorption capacity of the residues resulted comparable to that of limestone, and steadily increased for a significant number of cycles. This peculiar behavior was attributed to the presence of a chlorinated phase which enhances the CO_2 uptake in the diffusion-controlled stage of carbonation, by reducing the product layer resistance to CO_2 diffusion. No significant release of acid gases was observed at the characteristic temperatures of calcium looping carbonation.

1. INTRODUCTION

There is overwhelming consensus in the scientific community that the global warming that our planet has been experiencing since the mid-20th century has an anthropogenic cause, namely the emission of greenhouse gases as carbon dioxide.[1] Despite the remarkable progress of renewable energies, fossil fuel consumption worldwide is still increasing year-by-year.[2] Therefore, in order to achieve a meaningful reduction of CO_2 emissions in the near term, the deployment of a direct emission mitigation approach such as industrial CO_2 capture and storage (CCS) is considered as an option.[3]

Among the several CCS techniques proposed to realize pre- or post-combustion CO_2 capture processes, the so-called *Calcium Looping* scheme (CaL, detailed in section S1 of the Supplementary Information, SI), is based on the reversible reaction between calcium oxide (CaO) and CO_2 to form calcium carbonate ($CaCO_3$):[4-6]

$$CaO + CO_2 \leftrightarrow CaCO_3 \qquad \Delta H^0_{298\,K} = -178\ kJ\ mol^{-1} \qquad \text{R1}$$

The techno-economic prospects of the CaL process appear promising in comparison to the benchmark amine-based capture systems.[7] However, the CO_2 capture capacity of CaO derived from natural sources such as limestone rapidly decreases with repeated carbonation and calcination cycles. Attenuating this fast deactivation rate would be a boon to the commercial viability of the process.[8,9]

Although several investigators focused on the modification of Ca-based sorbents via diverse synthesis routes,[9] the feasibility of this capture technology relies on the cheapness of the sorbent, and most of the complex methods of sorbent modification proposed will be prohibitively expensive for scale-up.[10,11] Conversely, the use of waste materials as sorbents or precursors for modified sorbents could represent a potential route for achieving cost-effective improvement of performance. Various Ca-based waste materials have been screened as CO_2 sorbents, *e.g.* carbide slag from the chlor-alkali industry,[12] lime mud from paper manufacturing[13] and waste eggshells.[14]

Dry processes for acid gas removal from flue gas generated in waste-to-energy (WtE) facilities generate relevant amounts of solid alkaline wastes, known as air pollution control (APC) residues. APC residues usually amount to 2-5% by mass of the original waste on a wet basis[15] and their composition mainly depends on the process adopted for the abatement of the acid compounds (*e.g.* HCl, SO_2) present in flue gases. A widespread technique is the injection of calcium hydroxide, $Ca(OH)_2$, into the flue gas stream.[16,17] The Ca-based APC residues resulting from the reaction between $Ca(OH)_2$ and the acid pollutants, specifically known as residual calcium chemicals (RCC), still present a high content of available calcium,[18] although mixed

with reaction products and with a relevant fraction of fly ash. To date, despite increasing research efforts to develop alternative RCC management routes,[19] the usual fate of Ca-based residues from WtE plants is landfilling.[20] The related environmental burden is relevant: RCCs carry a fly ash fraction containing a variety of heavy metals in traces. Moreover, the presence of unreacted $Ca(OH)_2$, giving high alkalinity, and the high content of chlorides, having metal complexing capacity, increases the potential for leaching of amphoteric trace metals.[21] As a result, Ca-based APC residues are generally classified as hazardous waste.[22,23] Thus, in light of both health concerns and of the principles of circular economy, processes for the recycle or reuse of RCC is a key issue to improve the overall sustainability of WtE flue gas cleaning systems.[24]

Gas-solid carbonation has already been proposed as a method for the safe disposal of RCCs.[25] Instead of landfilling the solid residue "as is", the RCCs are contacted with a gas stream containing CO_2 at high temperature. Carbonation reduces the solubility of RCC[26] and decreases the mobility of trace metals as Cu and Zn, present in the fly ash fractions,[27,28] thus producing a residue that is less prone to leaching.[29] The improvement observed in the environmental stability of RCC ensures safer disposal, yet it appears not to be a sufficient driver to persuade WtE operators to invest in the accelerated carbonation process.

In the present study, the integration of the gas-solid carbonation of RCCs in the CaL framework is considered, *i.e.* exposing RCCs to repeated carbonation/calcination cycles. If carbonation of RCC waste streams could be effectively performed upon multiple cycles, the accelerated carbonation approach would change from a pre-treatment before disposal to an actual route to the valorization of the RCCs. RCCs could be considered an alternative feedstock to limestone in the CaL process, as outlined in Figure 1. The viability of this route could contribute to the

deployment of CCS schemes directly in waste-to-energy plants, where recent studies evidenced the potential for achieving negative CO_2 emission, still hindered by relevant cost barriers.[30]

In the following, the carbonation behavior of RCC samples collected from different WtE plants is compared to that of a reference limestone, in order to present a preliminary screening of the re-use of RCCs in CaL applications. The CO_2 capture characteristics of the residues are discussed in light of a detailed characterization of the fresh materials and of an analysis of their performance in cyclic operation.

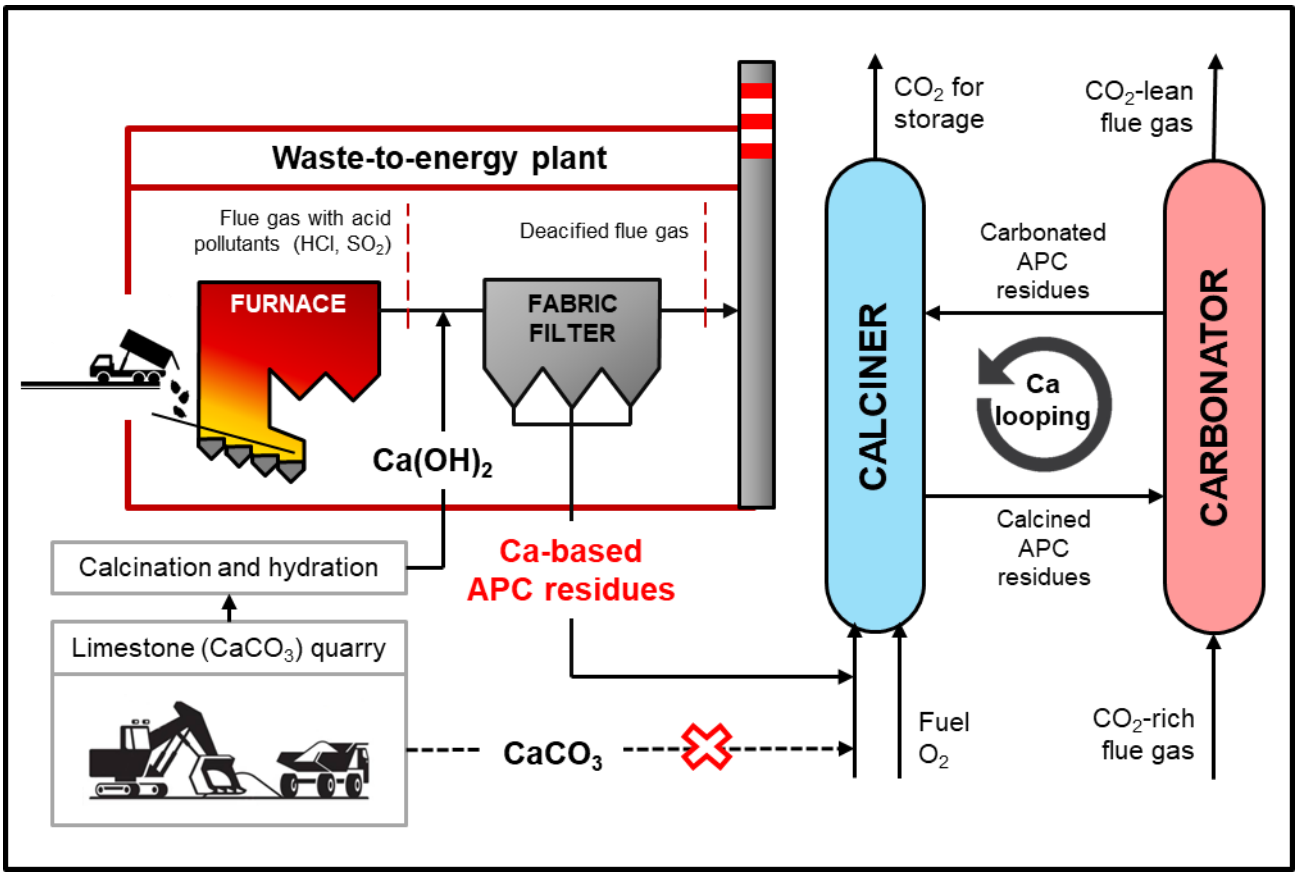

Figure 1. The use of Ca-based APC residues from WtE flue gas cleaning as alternative feedstock for the calcium looping process, in substitution of limestone.

2. MATERIALS AND METHODS

2.1. Materials. Solid residues (RCC) of the process of dry acid gas removal with powdered hydrated lime were sampled in three different waste-to-energy plants in Northern Italy, from the solid stream leaving the baghouse section located downstream of the lime injection point. The virgin commercial lime (96% $Ca(OH)_2$, the balance being $CaCO_3$) before injection was also collected. The samples were then homogenized by quartering, prior to subsequent analysis.

A short description of the dry sorbent injection (DSI) process that originated the residues is reported in section S2 of the SI, alongside the average flue gas composition in the three plants. DSI has the objective to neutralize the acid pollutants HCl and SO_2 (typically present in the raw flue gas of WtE plants in concentrations of 700-1200 mg/Nm^3 and 20-100 mg/Nm^3, respectively). Further details on the process are reported in the literature.[31-33]

Synthetic mixtures of lime, fly ash and calcium chloride ($CaCl_2$) were prepared by means of simple mechanical mixing in a mortar for 5 min. $CaCl_2$ was a reagent grade chemical (Sigma-Aldrich), while Ca-free fly ash was sampled in one of the three WtE plants, from the discharge of a superheater device, upstream of the $Ca(OH)_2$ injection point. Natural limestone rock (99% $CaCO_3$) from a German quarry[34] was used as reference material.

2.2. Experimental Techniques. The crystallinity and chemical composition of materials were determined using X-ray powder diffraction. The diffractometer, a PANalytical Empyrean equipped with a Bragg-Brentano HD mirror, was operated at 45 kV and 40 mA using CuKα radiation (λ = 1.5418 nm). Each sample was scanned in the 2θ range of 20-80°. The step size was 0.016° and the scan time per step was 0.68 s.

A high-resolution digital field emission scanning electron microscope (FE-SEM), Zeiss Ultra 55 plus, was used to visualize the materials before and after thermogravimetric runs. Prior to imaging, the samples, placed on a conductive carbon tape, were sputter-coated by gold/palladium (Au/Pd) for 90 s under Ar plasma to improve their conductivity (BAL-TEC SCD-050). Additionally, for the elemental mapping of Ca, S, and Cl in the materials, a Leo Gemini 1530 SEM equipped with an energy dispersive X-ray spectrometer (EDX) was used.

Thermogravimetric (TG) runs were carried out using a TGA-Q500, TA Instruments thermal analyzer. Procedures and conditions of different experimental runs are described in section 2.3.

A Netzsch STA 409/C thermoanalyzer and a Bruker Equinox 55 FTIR spectrometer (equipped with MCT detector and a gas cell), coupled by means of a heated PTFE transfer line to avoid the condensation of decomposition products was used to carry out simultaneous TG-FTIR measurements.

2.3. Procedures. Thermal stability and weight loss with respect to temperatures of samples were investigated by TG runs consisting in a drying step (isotherm at 105 °C for 10 min in inert atmosphere: 60 mL/min of N_2 sample flow and 40 mL/min of N_2 balance flow) followed by a heating ramp to 900 °C at a constant rate of 10 °C/min in N_2 atmosphere.

The TG analyzer was used also to explore the carbonation behavior of the RCC samples. The following procedure was applied:

- pre-calcination step (also mentioned in the following text as activation): a sample weight of about 20 mg and a platinum pan were selected. The sample was heated from

ambient to 800 °C at a rate of 50 °C/min in inert atmosphere (60 mL/min of N_2 sample flow and 40 mL/min of N_2 balance flow).

- carbonation/calcination loops: after the pre-calcination step, the sample was cooled at the desired temperature for carbonation and the sample flow was switched to 60 mL/min of CO_2, in order to perform the carbonation reaction in an atmosphere containing 60 vol.% CO_2 (the rest being N_2 balance flow) for 20 min. Subsequently, regeneration of the sorbent via calcination was performed by switching the sample flow to 60 mL/min of N_2 and heating the sample up to 900 °C for 10 min. The carbonation and calcination cycle was repeated 10 or 20 times.

TG-FTIR experimental runs were carried out using a pure N_2 purge flow (60 mL/min) at a constant heating rate of 20 °C/min. The time resolution of IR spectra collection was of 9.7 s, more than sufficient to capture the gas evolution rates characteristic of TG runs at the adopted heating rate.[35] The wavenumber intervals used to extract the emission profiles for the different gas species were the following: 4025-3792 cm^{-1} for H_2O, 2971-2952 cm^{-1} for HCl, 2400-2240 cm^{-1} for CO_2, 1425-1280 cm^{-1} for SO_2. The 30 s residence time calculated for the gas in the transfer line was used to correct the time delay between TG and IR results.

3. RESULTS

3.1. Characterization of Residues. The elemental composition of the three RCC samples considered is reported in Table 1. As expected, calcium is the most abundant element in RCCs, being these powders the residues of the injection of hydrated lime in the flue gas. However, a variety of other species (Si, Mg, K, Na, Zn, Al, Fe) are also present in the samples, due to their presence in fly ash. Chlorides and sulfates result from the reaction of hydrated lime with HCl and

SO_2 present in the flue gas. Typically, the concentration of HCl in WtE untreated flue gases is about an order of magnitude higher than that of SO_2.[36,37] In Figure 2, the SEM-EDX elemental map of the RCC-FC sample shows that chlorides and sulfates are quite homogeneously distributed in the sample and confirms a higher abundance of Cl over S (21.9 over 3.1 atomic %).

Table 1. Concentration of the main components in the three RCC samples (g/kg dry mass).

Element	RCC-FC	RCC-FE	RCC-RN
Metals [a]			
Calcium	360.0 ± 130.7	324.0 ± 149.2	339.0 ± 155.8
Silicon	124.9 ± 40.1	127.7 ± 43.3	175.6 ± 55.2
Magnesium	8.1 ± 1.9	8.6 ± 2.0	23.3 ± 5.6
Potassium	37.3 ± 17.2	26.8 ± 12.3	18.2 ± 8.4
Sodium	31.4 ± 14.1	27.9 ± 12.5	13.6 ± 6.1
Zinc	6.6 ± 1.5	11.7 ± 2.7	7.8 ± 1.8
Aluminum	14.7 ± 6.3	16.7 ± 7.2	7.4 ± 2.8
Iron	6.1 ± 1.5	10.2 ± 2.5	3.8 ± 0.9
Inorganic compounds [b]			
Chlorides	148.0 ± 23.5	155.0 ± 24.6	122.0 ± 19.4
Sulfates	15.8 ± 1.2	19.4 ± 1.5	11.8 ± 9.0

[a] tested according to UNI EN 13657:2004 + UNI EN ISO 11885:2009

[b] tested according to EPA 300.0 1993

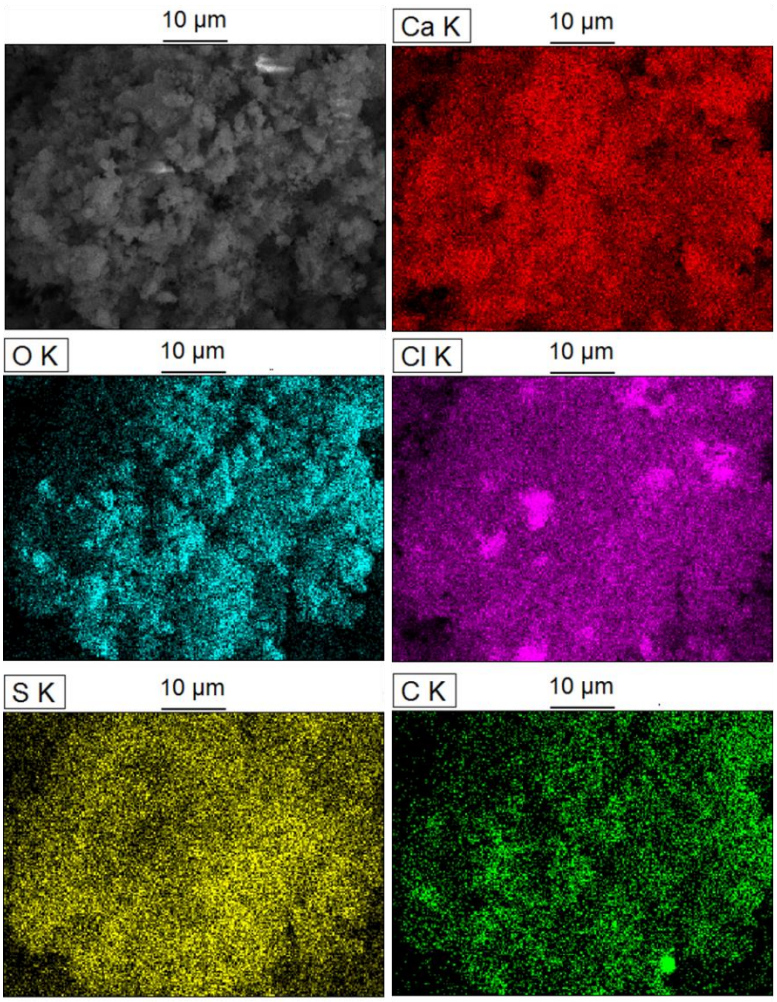

Figure 2. SEM image of the RCC-FC sample and K-edge elemental maps of Ca, O, Cl, S and C.

X-ray diffraction allowed determining the mineral composition of the samples. Figure 3 shows the XRD patterns of the RCC samples compared to that of the virgin commercial hydrated lime. The latter is composed of portlandite, $Ca(OH)_2$, with $CaCO_3$ impurities in the form of calcite. The RCC samples contain unreacted $Ca(OH)_2$, CaOHCl as product of the reaction with HCl and $CaSO_4$ as main product of the reaction with SO_2. $CaCO_3$ is present in the form of aragonite, which is the preferred form generated in presence of chloride,[38] in addition to the calcite already observed in the virgin lime. The main crystalline species for the fly ash fraction are NaCl, KCl, SiO_2 and MgO.

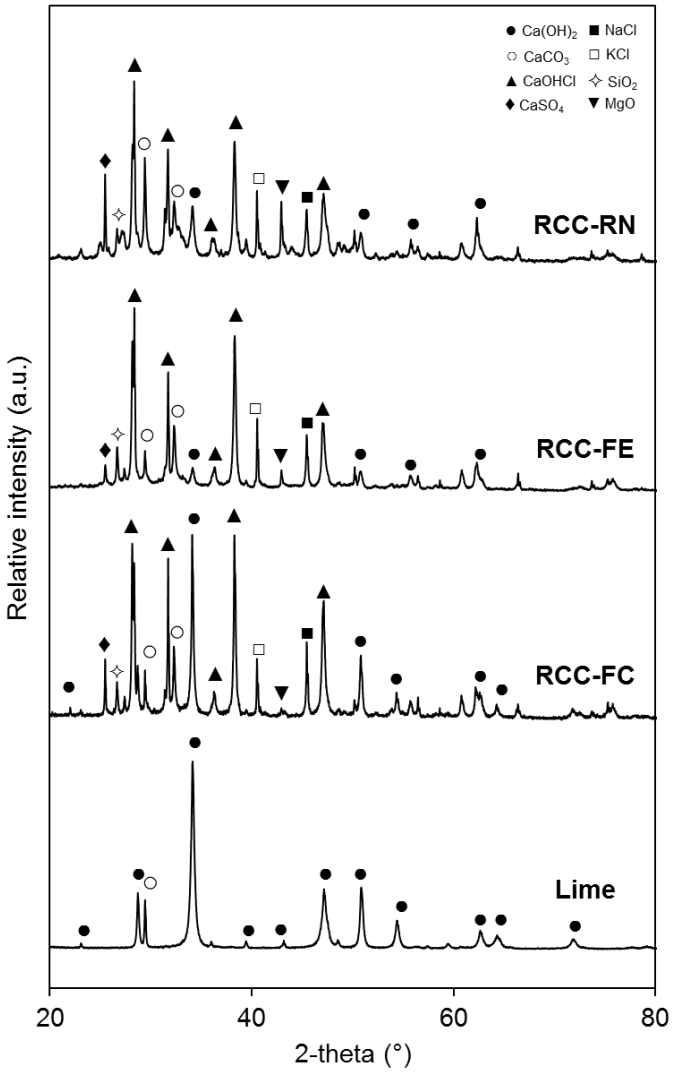

Figure 3. X-ray patterns of a commercial lime sample and of the three RCC samples.

The morphology of the samples is shown in the SEM micrographs of Figure 4. The roughly hexagonal plate-shaped nano-grains, typical of portlandite,[39] obviously dominate in virgin lime. These can be still spotted in the RCC samples, confirming the presence of unreacted $Ca(OH)_2$. However, $Ca(OH)_2$ nano-grains are mostly covered by a rather uniform product layer of $CaCO_3$, particularly evident in Figure 4c, and in Figure 4b, where they are mixed with elongated, laminar crystals attributable to the chlorinated phase.[40]

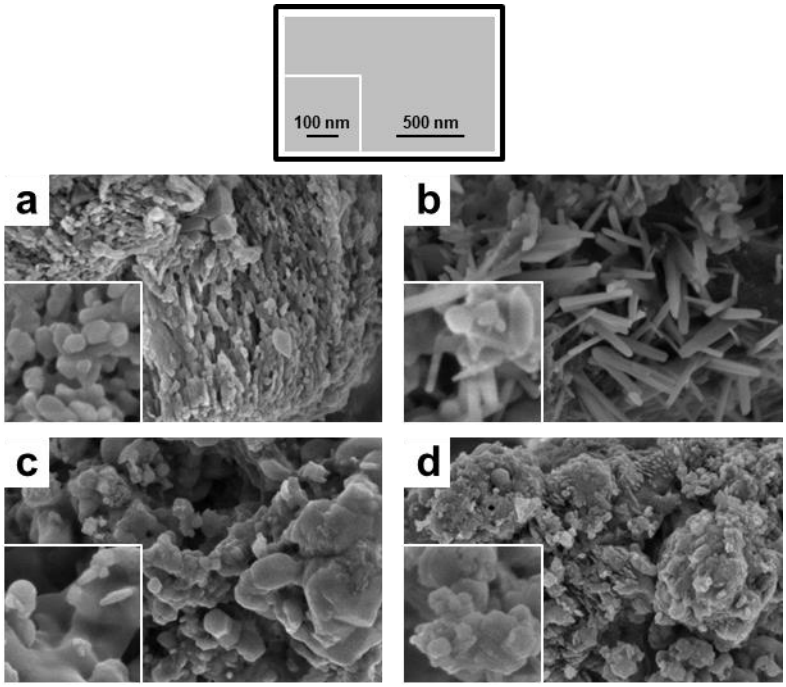

Figure 4. Morphology of the samples "as received": a) commercial lime, b) RCC-FC, c) RRC-FE, and d) RCC-RN.

Thermal decomposition of the samples via TGA/DTG analyses was used to obtain quantitative information about the Ca-containing phases identified via XRD. As shown in Figure 5, the derivative weight loss curve pinpoints the presence of the main components thanks to their well-distinguished decomposition temperatures. The dehydration of unreacted $Ca(OH)_2$ to CaO takes place in the interval 350-400 °C:[41]

$$Ca(OH)_2 \rightarrow CaO + H_2O \qquad \text{R2}$$

CaOHCl decomposes to $CaCl_2$ and CaO at 450-550 °C:[42,43]

$$2\ CaOHCl \rightarrow CaO + CaCl_2 + H_2O \qquad \text{R3}$$

$CaCO_3$ decomposes to CaO at temperatures higher than 600 °C:[44]

$$CaCO_3 \rightarrow CaO + CO_2$$ R4

The sulfate phases ($CaSO_3$ and $CaSO_4$) undergo slow decomposition processes at temperatures higher than 800 °C, in agreement with Bogush et al.[45] The resulting DTG profiles resemble those shown in previous reports on the composition of APC residues.[25,45,46]

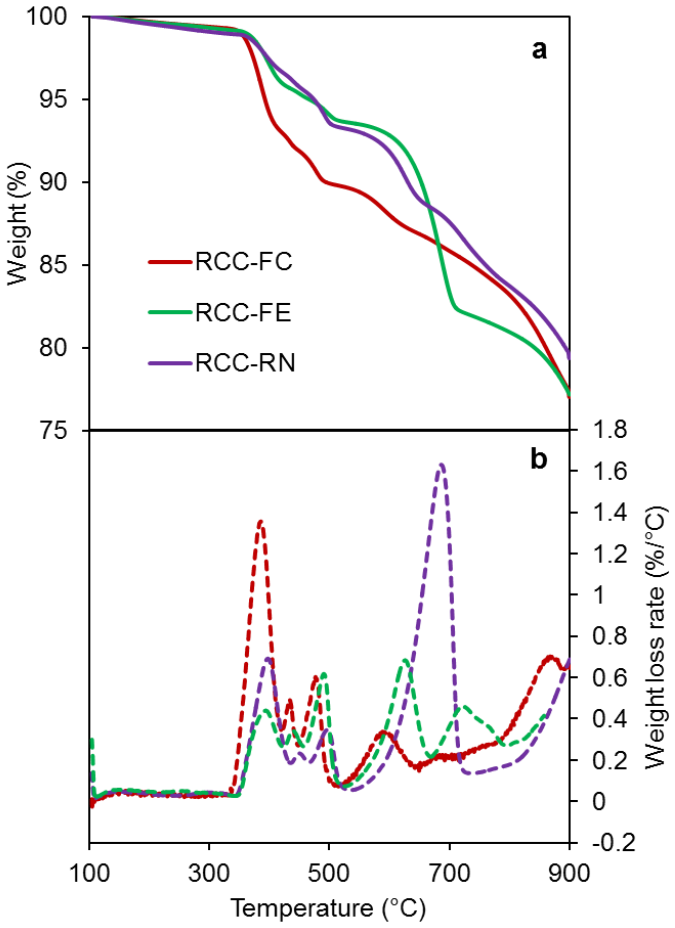

Figure 5. a) Weight loss and b) weight loss rate curves for the three RCC samples. TG runs were carried out at 10 °C/min constant heating rate and in 100 mL/min pure nitrogen flow.

By attributing the weight loss steps recorded in TG runs to the related reaction processes, the partitioning of Ca in the sample among $Ca(OH)_2$, CaOHCl and $CaCO_3$ was calculated, assuming that sulfated species and fly ash constitute the residual weight of the sample (see Table 2). The

results of the calculation provide the amount of Ca available for the carbonation process, *i.e.* Ca in the form of CaO after the activation of residues at 800 °C. Ca-based carbonatable species constitute approximately 70-80% of the total mass of the samples, in line with previous data on APC residues.[47] The high amount of $Ca(OH)_2$ in the RCC-FC sample and the low amount of CaOHCl in the RCC-RN resulting from the calculation are in agreement with the relative intensity of the respective peaks in the XRD patterns shown in Figure 3.

Table 2. Mass fraction (wt.%) of the main species in the untreated and calcined RCC samples.

	RCC-FC		RCC-FE		RCC-RN	
Compound	Fresh	Calcined	Fresh	Calcined	Fresh	Calcined
$Ca(OH)_2$	23.4	-	7.5		14.5	-
CaOHCl	35.2	-	36.4		20.9	-
$CaCO_3$	23.1	-	31.0		39.6	-
CaO	-	51.1	-	42.0	-	51.3
$CaCl_2$	-	26.1	-	27.0	-	16.3
Sulfated phases + fly ash	18.4	22.8	25.1	31.0	25.0	32.4
$CaCl_2$ in the Ca fraction		33.8		39.1		24.0

The information gathered from the TG runs was complemented with a TG-FTIR analysis to investigate the evolved gases generated during the thermal decomposition of the residues. Figure 6 reports the results of a TG-FTIR run for the RCC-FC sample. The release of H_2O and CO_2 respectively in the temperature ranges between 400-600 °C and 600-800 °C further confirms the occurrence of reactions R2-3 and R4 respectively in the first and second temperature interval. More interestingly, TG-FTIR allowed the identification of the temperatures at which the release

of HCl and SO_2 becomes significant. HCl starts being detected at temperatures higher than 900 °C, where presumably the calcium chloride formed in reaction R3 is decomposed, while a detectable evolution of SO_2 from the sample started at 800 °C. Since pure $CaSO_4$ decomposes only at temperatures higher than 1300 °C,[48] this emission might be attributed to $CaSO_3$, which in the absence of oxygen can decompose at temperatures as low as 850 °C.[49] Figure S2 in the SI shows the limited effect of the release of SO_2 in terms of weight loss of a RCC sample during a typical cyclic TG run as those presented in section 3.3.

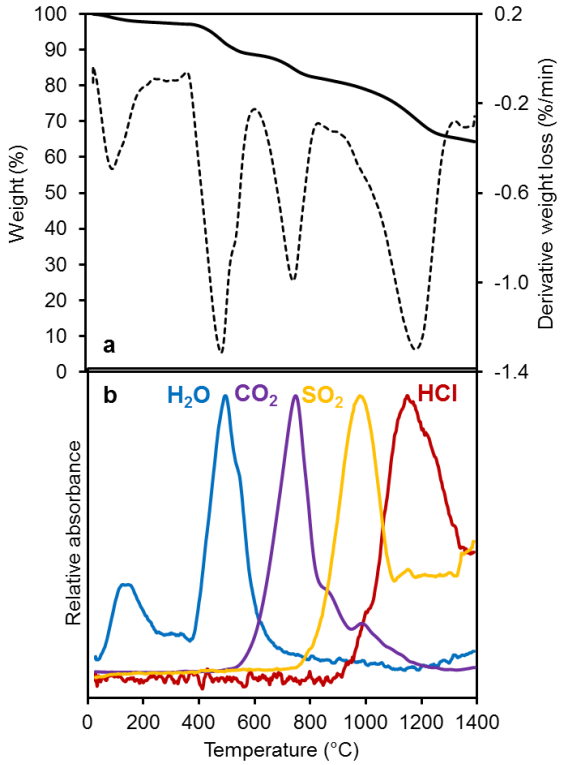

Figure 6. Results of a TG-FTIR run performed on a RCC-FC sample. (a) TG and dTG curves of the sample in pure nitrogen (20 °C/min heating rate); (b) qualitative emission profiles of H_2O, CO_2, SO_2 and HCl in nitrogen, normalized with respect to the most intense absorbance peak for each gas.

3.2. Carbonation. Experimental TG runs to test the carbonation of RCC samples were performed at different temperatures under 60 vol.% CO_2 after pre-calcining the samples at 800 °C in N_2 atmosphere. The results of the carbonation tests are reported in Figure 7. The figure shows the increase in the weight of the sample due to the progress of the carbonation reaction. Figure 7a compares the CO_2 sequestration curves of the RCC-FC sample at 500, 600 and 700 °C with those carried out at the same temperatures on the natural limestone sample selected as a reference. Figure 7b compares the CO_2 uptake curves of all the three RCC samples at 700 °C.

The shape of the kinetics curves clearly shows the two reaction stages in which the carbonation reaction can be divided:[50] (i) an initial fast kinetically-controlled stage, where the chemical reaction is extremely rapid and $CaCO_3$ crystals form a solid product shell filling the pores of lime, followed by (ii) a slow conversion stage, controlled by the sluggish diffusion of CO_2 through the product layer.

The calcium conversion of the samples can be calculated from the uptake of CO_2, given the amounts of CaO in the activated RCC samples (Table 2). At 700 °C the RCC-RN sample exhibited the highest conversion (81.3%), followed by RCC-FC (63.1%), while only 50.1% of the available CaO in RCC-FE was converted. The wide range of conversions reflects the variety of the behavior of RCC materials, already observed in previous studies. Baciocchi et al.[25] performed the gas-solid carbonation of Ca-based residues in pure CO_2 in the temperature range 200-500 °C, reporting a maximum calcium conversion of 57% at 400 °C, corresponding to a storage capacity of 0.12 g of CO_2/g of sorbent. Prigiobbe et al.[43] carbonated APC residues in the interval 350-500 °C under CO_2 concentration ranging from 10 to 50 vol.%, observing maximum conversions comprised between 60 and 80%. Tian and Jiang[51] reported gas-solid carbonation results with 10 vol.% concentration of CO_2, obtaining conversions between 68.6 and 77.1%.

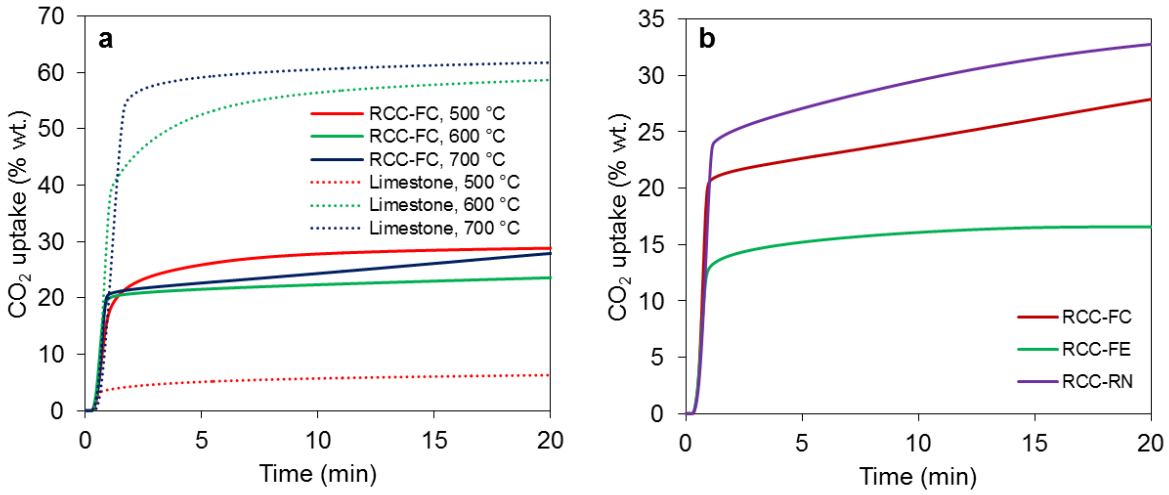

Figure 7. a) CO_2 sequestration curve of RCC-FC at different temperatures under 60 vol.% CO_2, compared to the reference limestone. Pre-calcination at 800 °C in N_2. b) CO_2 sequestration curve of the three RCC samples at 700 °C under 60 vol.% CO_2, after pre-calcination in N_2 at 800 °C.

The morphology of samples after the activation step and after carbonation was investigated via electron microscopy. The results are shown in Figure 8. As discussed in section 3.1, the pre-calcination at 800 °C triggers reactions R2-4, generating CaO available for carbonation and increasing the porosity of the samples, compared to that of the "as received" materials of Figure 4. After carbonation, the samples are covered by a $CaCO_3$ product layer. The coverage degree qualitatively confirms the calculated calcium conversion: a uniform carbonate shell covers most of the surface of the highly converted RCC-RN sample, while the least converted sample (RCC-FE) still shows an open porous structure, although the size of its grains is inflated by $CaCO_3$ growth.

3.3. Cyclic Performance. Figure 9 shows the cyclic CO_2 capture performance of the RCC residues, expressed in terms of mass CO_2 uptake (g of adsorbed CO_2/g of calcined sorbent) at the end of each TG carbonation run. The figure also reports the performances of the unconverted

commercial lime originating the RCCs, and of a commercial limestone, selected as a reference material. The same data are shown in terms of conversion of available CaO in Figure S3 of the SI (see Table 2 for the mass fraction of CaO in the calcined RCCs). A carbonation temperature of 700 °C was chosen, in order to maximize CO_2 capture (cyclic tests with carbonation temperatures of 500 °C and 600 °C are reported in Figure S4 of the SI, with reference to the RCC-FC sample).

As expected, limestone exhibits a high initial CO_2 uptake (0.64 g CO_2/g sorbent), which steadily declines during cycling. A value of 0.28 g CO_2/g sorbent (43% of the initial value) is obtained after 10 cycles. Fresh commercial calcium hydroxide (lime) behaves similarly. The CO_2 uptake in the 1st cycle is slightly lower than for the limestone reference sample considered (0.55 g CO_2/g sorbent), in agreement with the fact that CaO derived from $Ca(OH)_2$ dehydration tends to be less porous than CaO obtained from $CaCO_3$ calcination.[52] However, in the following cycles the performance is almost correspondent to that of limestone, and the same quantitative performance is obtained after 10 cycles, *i.e.* the characteristic monotonic decline of CO_2 uptake due to sorbent sintering.

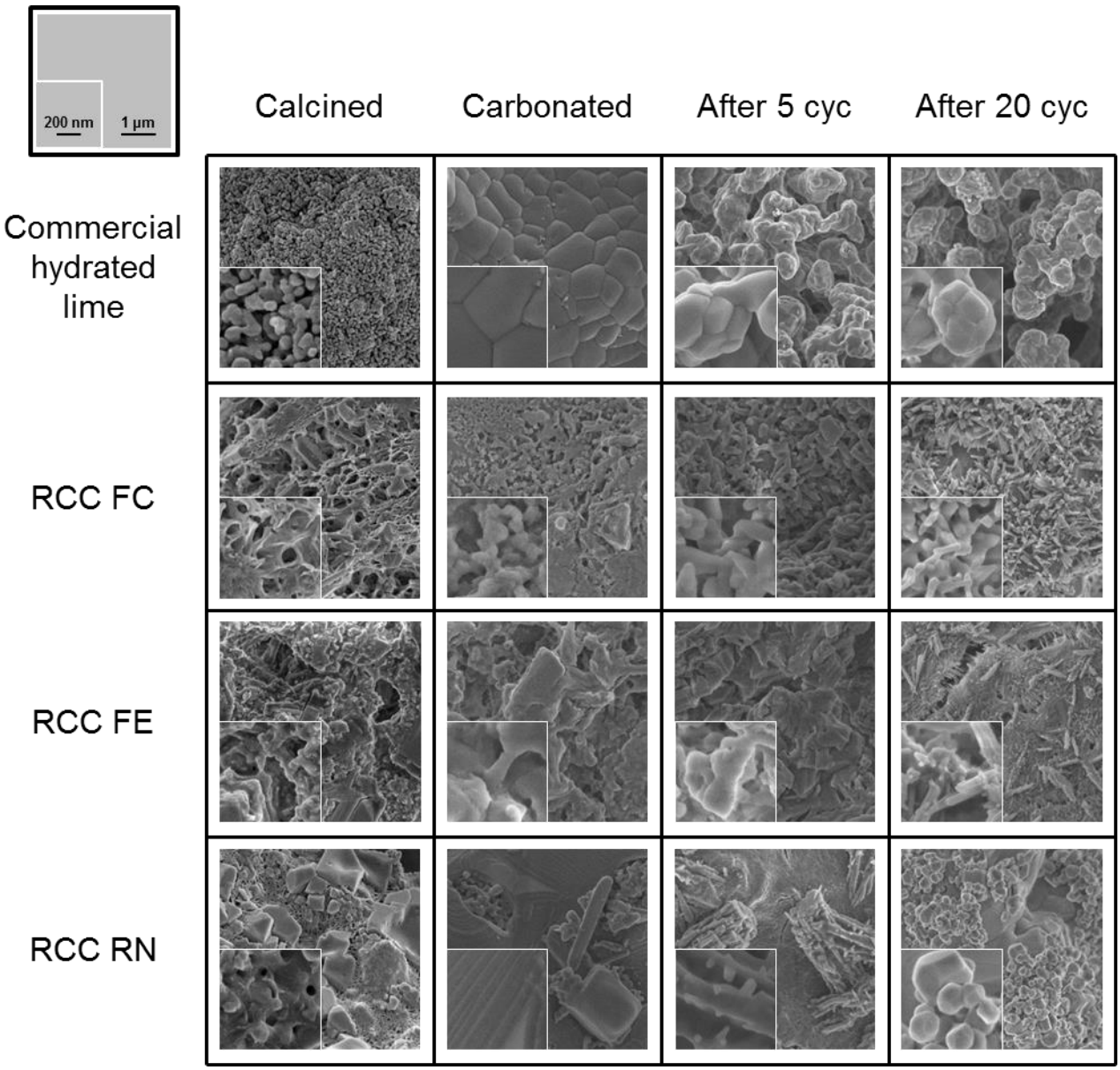

Figure 8. SEM micrographs of "fresh" commercial lime and RCC samples during testing: after the pre-calcination step at 800 °C, after 1st carbonation (carbonated form), after 5 cycles (calcined form), after 20 cycles (calcined form). Carbonation performed at 700 °C, 60 vol.% CO_2 in N_2.

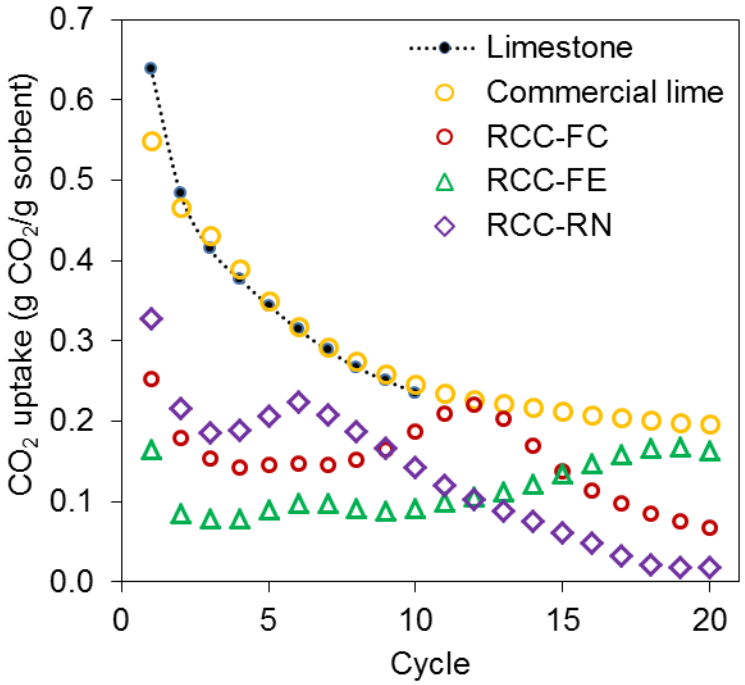

Figure 9. CO_2 uptake over 20 cycles of carbonation (700 °C, 60 vol.% CO_2 in N_2) and calcination (900 °C, 100% N_2) for the three activated RCC samples, compared to "fresh" commercial lime and to the natural limestone selected as a reference.

The three samples of RCC show widely different behaviors. The RCC-FC shows an initial uptake of 0.25 g CO_2/g sorbent, quickly stabilizes its sorption capacity at a value of 0.14 g CO_2/g sorbent for 6 cycles and then exhibits a remarkable resurgence of performance which brings its 12-cycle uptake at 0.22 g CO_2/g sorbent, before decaying to a 20th-cycle value of 0.07 g CO_2/g sorbent. The CO_2 uptake of RCC-RN in the 1st-cycle is quite high, with a value of 0.33 g CO_2/g sorbent, then declines for the following two cycles, shows a performance recovery peaking at 0.22 g CO_2/g sorbent in cycle 6, before steadily declining to the value of 0.02 g CO_2/g sorbent after 20 cycles. Finally, RCC-FE shows a very low uptake in the 1st-cycle (0.17 g CO_2/g sorbent), but, after a marked decline in the first 3 cycles, its capture capacity constantly raises, ending in an uptake of 0.16 g CO_2/g sorbent after 20 cycles.

Despite the differences among the specific RCC samples, it is worth noticing that the decay profiles of the RCC samples all have three common elements, evident at different times and with different intensities for the three samples: a fast rate of decay during the first 3 cycles followed by an uptick of performance and by a gradual performance decline after a high number of cycles.

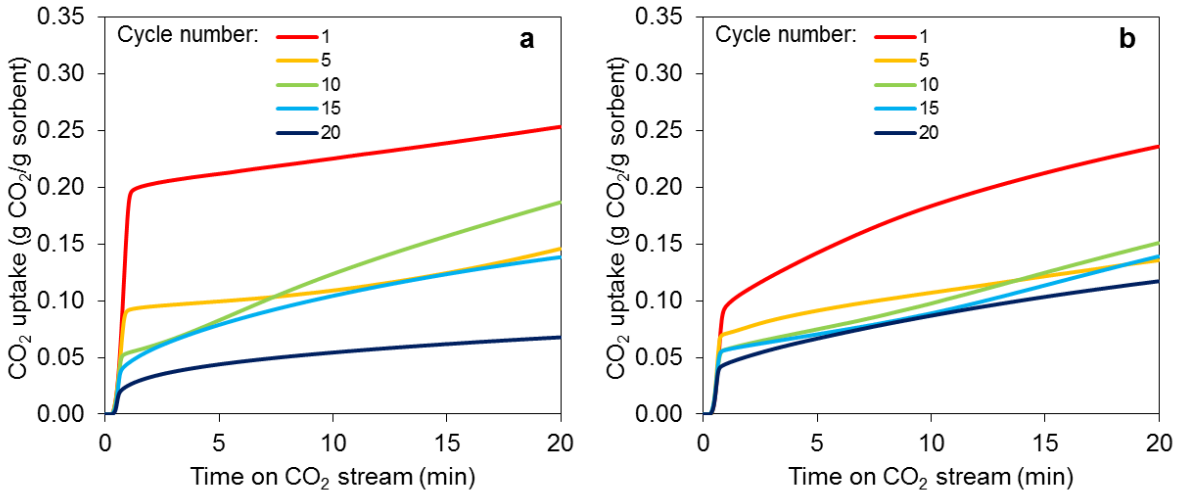

Figure 10. CO_2 sequestration curve during different cycles for: a) RCC-FC sample, b) mixture of commercial lime and $CaCl_2$ (weight ratio 70:30). Cycling conditions as in Figure 9.

A more detailed assessment of the evolution of the CO_2 uptake as a function of time during cycling allows gaining further insights on the peculiar behavior of RCCs. Figure 10a shows the kinetics of CO_2 sequestration at different cycle numbers for the RCC-FC sample. The two stages of the carbonation reaction identified in section 3.2 evolve differently as cycling proceeds. The CO_2 uptake during the fast kinetically-controlled stage (1st minute of reaction) decreases monotonically with cycle number. Since the fast reaction regime is supposed to be governed by the filling of small pores,[53] an earlier occurrence of the transition between the fast and slow stages of reaction as a consequence of cycling is a predictable effect of the sintering of the Ca-based compounds. Conversely, the CO_2 uptake during the subsequent slow diffusion-controlled

stage first increases and then decreases with cycle number, giving rise to the peculiar decay profile observed in Figure 9.

The SEM images of Figure 8 document the evolution of the morphology of samples in calcined form during cycling. Commercial lime provides a visual reference of the effect of sintering in inflating CaO grain size and disrupting the mesoporous structure of the original activated material. RCC samples exhibit a more complex morphology than pure lime, owing to the presence of impurities and phases melting during cycling, as $CaCl_2$, which modify the aspect of samples. However, the micrographs at higher magnification in the insets appear to indicate that all samples suffered some sintering with respect to the original activated material. Nevertheless, RCC-FC and RCC-FE samples retained a more open porous structure after cycling than RCC-RN, in agreement with TG results that evidence a more pronounced performance decay of the latter sample.

3.4. Analysis of the RCC Behavior upon Cycling. In order to understand which component in the RCC samples determines the behavior of RCC observed in Figure 9, synthetic mixtures of commercial lime and calcium chloride, and of commercial lime and fly ash in different mass ratios were tested in the TG analyzer under the same conditions used for RCCs. The RCCs after pre-calcination at 800 °C are mainly composed of CaO, $CaCl_2$ and of the fly ash fraction. Thus, experimental tests carried out with the two mixtures were aimed at excluding one of the three macro-components of RCC, to verify if the interplay between the other two replicates the qualitative behavior observed for the RCC samples.

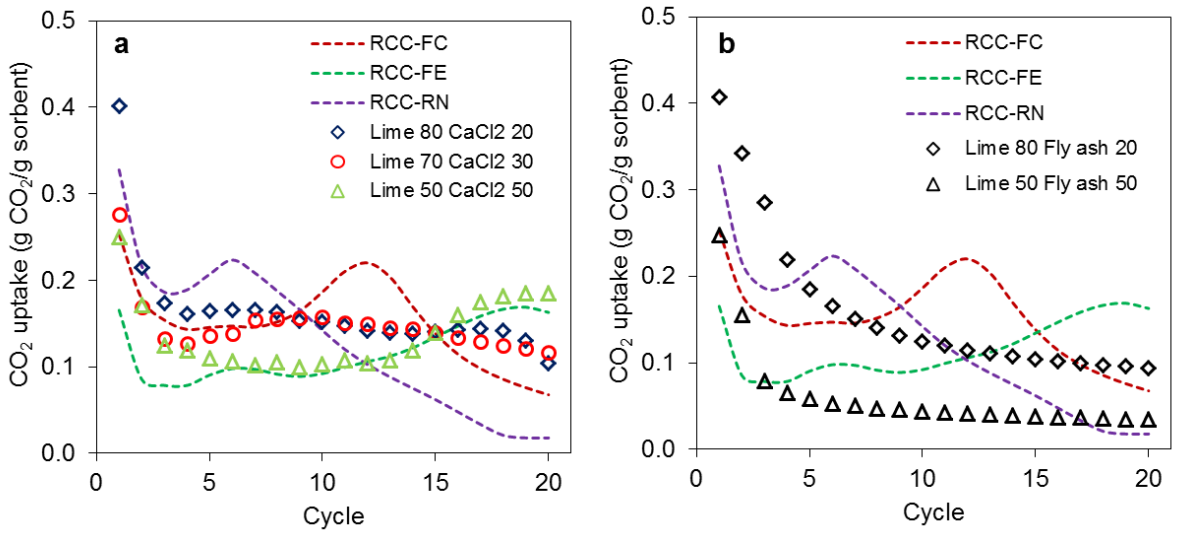

Figure 11. CO_2 uptake over 20 cycles of carbonation (700 °C, 60 vol.% CO_2 in N_2) and calcination (900 °C, 100% N_2) of: a) mixture of commercial lime and $CaCl_2$, and b) mixture of commercial lime and fly ash in the reported mass ratio, compared to the performance of RCC samples.

The cycling performance of the mixtures is reported in Figure 11, where a comparison with that observed for RCCs is possible. Mixing lime with 20 or 50 wt.% fly ash results in a sorbent with a monotonically decreasing CO_2 sequestration over cycling. Conversely, the mixtures of lime and $CaCl_2$ exhibit complex trajectories of performance over cycling. The mixture with 30 wt.% $CaCl_2$ shows a trend comparable to the CO_2 capture profile of the RCC-FC sample (composed by 34 wt.% of $CaCl_2$ as shown in Table 2) at least for the first 8 cycles, presenting a maximum performance at cycle 9 before a steady decrease of sorption capacity. The mixture with 50 wt.% $CaCl_2$ shows a marked improvement of CO_2 uptake in the last 7 cycles, similarly to the RCC-FE sample (39% $CaCl_2$ as shown in Table 2). The mixture with 20 wt.% $CaCl_2$ shows a small uptick in performance at the 5^{th} and 6^{th} cycles, before exhibiting a constant decline of sorption capacity, in line with the behavior of RCC-RN (24% $CaCl_2$). Despite the synthetic mixtures cannot exactly

reproduce the irregular behavior of RCC samples, the addition of $CaCl_2$ to the virgin lime replicates the observed increased performance over cycling, while the addition of fly ash simply dilutes the amount of calcium available for carbonation in the sorbent, resulting in a lower, constantly decreasing CO_2 capture capacity.

From the analysis of the results in Figure 11, it can thus be inferred that the $CaCl_2$ phase is arguably responsible for the partial recovery of CO_2 uptake during cycling showed by all the RCC samples. The comparison between the CO_2 capture curves during cycling of RCC-FC (Figure 10a) and of the mixture with 30 wt.% $CaCl_2$ (Figure 10b) allows highlighting their similar pattern in uptake recovery. This is evident in cycle 10, showing a higher final CO_2 sequestration than cycle 5 despite a lower uptake in the initial kinetic stage. This confirms that the presence of a chlorinated phase in the samples enhances the cyclic sorption of CO_2 during the diffusion-controlled stages of reaction.

The results obtained are in accordance with several previous studies. Gonzalez et al.[54] showed that doping limestone with KCl resulted in an increased rate of reaction in the slow carbonation phase. Al-Jeboori et al.[55] extended the investigation to various chloride salts, including $CaCl_2$, speculating that the presence of the Cl^- ion could enhance the ionic diffusion and mobility of carbonate ions through the $CaCO_3$ product layer, by straining the matrix. Similarly, a beneficial effect on reaction rate during the diffusion-controlled stage of carbonation was found for limestone doping with $CaBr_2$ by Manovic et al.[56]

In addition, several investigators recently reported on the positive effect of the presence of HCl on CO_2 capture in CaL conditions. Li et al.[57] showed that the discontinuous addition of HCl in the gas stream improves the cyclic CO_2 sequestration of limestone. The presence of moderate

amounts of CaOHCl in the carbonation products breaks the compactness of the $CaCO_3$ product layer, thus enhancing CO_2 diffusion through the layer,[58] as reported by Chin et al.[59] in their investigation on the sequential capture of CO_2 and HCl, although at much lower temperatures (200 °C). Wang et al.[60] observed a similar promoting effect of HCl toward limestone carbonation at least for a dozen of cycles. However, at a higher number of cycles, they reported the occurrence of a sharp decline in CO_2 sorption capacity, attributed to the possible formation of a thick $CaCO_3$-$CaCl_2$ molten phase (the eutectic mixture of these salts melts at 635 °C[61]), adverse to CO_2 diffusion.

Interpreting the experimental results obtained in the light of literature evidences, it can be assumed that the presence of the chlorinated solid phase in RCCs facilitates the product layer diffusion of CO_2, increasing the CO_2 sequestration during the diffusion-controlled regime of carbonation. The effect lasts for a few cycles and occurs at different cycle numbers depending on the amount of chlorides in the sample. After this effect ceases, the CO_2 sorption capacity appears to rapidly decrease, either due to the formation of a molten phase[60] or to the presence of Cl^- ions in the carbonate layer that aggravates sintering in the long run.[55]

4. DISCUSSION

The present investigation highlighted potentialities and weaknesses of the possible reuse of these residues in the CaL process based on a screening of the CO_2 sorption capacity of Ca-based APC residues over multiple carbonation/calcination cycles. The analyzed RCC samples showed a markedly lower initial CO_2 uptake than limestone, as a consequence of the lower amount of available calcium per mass of sorbent, but the decline in performance over a 20-cycle timespan was less pronounced, thanks to the effect of the chlorinated phase. However, while for limestone

most of the CO_2 sorption capacity is used in the first few minutes of kinetically-controlled carbonation even at high cycle numbers,[62] the appreciable CO_2 sequestration of RCC samples at late cycles benefits from a good carbonation performance during the whole time of the diffusion-controlled stage of reaction, as shown in Figure 10. In a fluidized bed environment, only part of this sorption capacity could be presumably harnessed during the short residence time in the carbonator vessel. Nevertheless, the chlorinated phase in RCCs not only enhances the CO_2 diffusion, but also promotes sintering, as evident from the compacting of RCC samples after cyclic TG runs (see Figure S5 in the SI). This is a beneficial effect when fluidized bed applications are considered. The tendency to sinter usually entails an increased resistance to attrition (the particle size reduction caused by the erosion of particles grinding together), which results in the loss of mass in a fluidized system via elutriation. Actually, the doping of limestone with chlorides has been suggested in literature to improve attrition resistance.[55]

A limitation of the present investigation is represented by the testing conditions in TGA. Although the data in Figure 9 provide a useful comparison of the behavior of different RCC samples to limestone, the CO_2 carrying capacity of RCCs has to be tested in harsher calcination conditions (higher temperature and CO_2-rich atmosphere) in order to simulate a realistic CaL process. Calcination at high CO_2 partial pressure is known to have detrimental effect on cylic CO2 uptake[63] and at higher temperature the presence of impurities, such as the fly ash fraction in RCCs, might trigger densification of CaO particles,[64] having again an adverse effect on the subsequent carbonation performance.

Another aspect that should be taken into account when considering RCCs as a feedstock for the CaL process is the potential release of harmful gases from the residues, which is a common issue in the thermal treatment methods for APC residue handling.[65] The TG-FTIR results obtained (see

Figure 6) may provide some preliminary information on this topic. The calciner vessel in a CaL scheme is expected to operate at temperatures of 900-950 °C,[66] thus the calcination of RCC samples may imply the release of SO_2 from $CaSO_3$, while the release of HCl should be minimal. The release of SO_2 in the calciner does not entail direct environmental consequences, because the CO_2-rich stream leaving the equipment is sent to geological storage. However, it can contribute to equipment corrosion. Nevertheless, it is worth recalling that the fuel burnt to heat the calciner (*e.g.* coal, as in the CaL pilot plants currently operating[5,67]) releases SO_2 itself in the CO_2-rich stream. In addition, if fresh RCCs are fed first into the carbonator, at 700 °C in a O_2-containing atmosphere, at least part of the $CaSO_3$ fraction can evolve to stable $CaSO_4$, which does not decompose at calciner temperatures, as mentioned in section 3.1 and as observed in the operational experience of CaL pilot plants.[68]

Eventually, beyond process operation, the reuse of RCCs has also to be considered from the economic and environmental points of view. Whereas limestone has a purchase cost, albeit low, RCCs are waste materials and WtE plants pay up to 200-300 €/t to send them to appropriate disposal sites.[69] Their use as a feedstock for CaL process may thus come at a virtually zero or even negative cost. Furthermore, the substitution of a natural resource such as limestone with a secondary material entails indirect environmental benefits. Considering a hypothetical medium-sized WtE plant equipped with DSI for acid gas removal and CaL for CCS, the amount of RCCs generated in the acid gas removal process would in principle allow to substitute up to 16% of the theoretical limestone feed required to capture 70% of the CO_2 emissions of the plant (see calculations in section S4 of the SI). In perspective, a detailed techno-economic analysis, which goes beyond the scope of the present study, may assess if the trade-off between the inferior CO_2

uptake performance of RCCs and their aforementioned advantages justifies the substitution of limestone feed in a CaL system.

5. CONCLUSIONS

The present study reported an experimental analysis of the potential of Ca-based residues generated by flue gas treatment in WtE plants as CO_2 sorbents in calcium looping applications. Despite the differences in composition and carbonation behavior, the three samples of residues from different plants tested in the study shared a specific CO_2 uptake trend over cycling, which does not decrease monotonically with cycle number as for limestone or the virgin commercial lime from which they are originated. After comparing the CO_2 sequestration of samples with that of synthetic mixtures of lime with $CaCl_2$ or fly ash, this behavior was ascribed to the presence of a relevant chlorinated phase in the samples, derived from the capture of HCl in WtE operation, which promotes the product layer diffusion of CO_2. The results obtained may contribute to explore the technical and economic feasibility of limestone feedstock substitution by RCCs in CaL processes.

ASSOCIATED CONTENT

Supporting Information.

The following files are available free of charge.

Brief description of the calcium looping process (section S1), brief description of the dry sorbent injection process (section S2), additional experimental data (section S3), preliminary estimate of limestone feed substitution (section S4) (PDF)

AUTHOR INFORMATION

Corresponding Author

* Tel. +39-051-2090240, Fax +39-051-2090247, e-mail: valerio.cozzani@unibo.it

Notes

The authors declare no competing financial interest.

ACKNOWLEDGMENT

The authors gratefully acknowledge Federica Barontini (University of Pisa, Italy) for the help with the TG-FTIR experiment. FIRST – Center for Micro- and Nanoscience at ETH Zürich is acknowledged for providing access to electron microscopy.

ABBREVIATIONS

APC, air pollution control; CaL, Calcium looping; CCS, CO_2 capture and storage; DSI, dry sorbent injection; RCC, residual calcium chemicals; WtE, waste-to-energy;

REFERENCES

(1) Cook, J.; Oreskes, N.; Doran, P.T.; Anderegg, W.R.; Verheggen, B.; Maibach, E.W.; Carlton, J.S.; Lewandowsky, S.; Skuce, A.G.; Green, S.A.; Nuccitelli, D.; Jacobs, P.; Richardson, M.; Winkler, B.; Painting, R.; Rice, K. Consensus on consensus: a synthesis of consensus estimates on human-caused global warming. *Environ. Res. Lett.* **2016**, 11 (4), 1-7.

(2) IEA, Key World Energy Statistics, International Energy Agency, technical report. Available at: www.iea.org/publications/freepublications/publication/key-world-energy-statistics.html (last accessed: 10/01/2018)

(3) IEA, World Energy Outlook 2017, technical report, OECD/IEA: Paris, 2008.

(4) Shimizu, T.; Hirama, T.; Hosoda, H.; Kitano, K.; Inagaki, M.; Tejima, K. A Twin Fluid-Bed Reactor for Removal of CO_2 from Combustion Processes. *Chem. Eng. Res. Des.* **1999**, 77, 62-68.

(5) Arias, B.; Diego, M.E.; Abanades, J.C.; Lorenzo, M.; Diaz, L.; Martinez, D.; Alvarez, J.; Sanchez-Biezma, A. Demonstration of steady state CO_2 capture in a 1.7 MW_{th} calcium looping pilot. *Int. J. Greenhouse Gas Control* **2013**, 18, 237-245.

(6) Abanades, J.C.; Arias, B.; Lyngfelt, A.; Mattisson, T.; Wiley, D.E.; Li, H.; Ho, M.T.; Mangano, E.; Brandani, S. Emerging CO_2 capture systems. *Int. J. Greenhouse Gas Control* **2015**, 40, 126-166.

(7) Zhao, M.; Minett, A.I.; Harris, A.T. A review of techno-economic models for the retrofitting of conventional pulverised-coal power plants for post-combustion capture (PCC) of CO_2. *Energy Environ. Sci.* **2013**, 6, 25-40.

(8) Diego, M.E.; Arias, B.; Mendez, A.; Lorenzo, M.; Diaz, L.; Sanchez-Biezma, A.; Abanades, J.C. Experimental testing of a sorbent reactivation process in La Pereda 1.7 MW_{th} calcium looping pilot plant. *Int. J. Greenhouse Gas Control* **2016**, 50, 14-22.

(9) Kierzkowska, A.M.; Pacciani, R.; Müller, C.R. CaO-based CO_2 sorbents: From fundamentals to the development of new, highly effective materials. *ChemSusChem* **2013**, 6, 1130-1148.

(10) Armutlulu, A.; Naeem, M.A.; Liu, H.-J.; Kim, S.M.; Kierzkowska, A.; Fedorov, A.; Müller, C.R. Multishelled CaO Microspheres Stabilized by Atomic Layer Deposition of Al_2O_3 for Enhanced CO_2 Capture Performance. *Adv. Mater.* **2017**, 29, 1702896.

(11) Erans, M.; Manovic, V.; Anthony, E.J. Calcium looping sorbents for CO_2 capture. *Appl. Energy* **2016**, 180, 722-742.

(12) Li, Y.; Sun, R.; Liu, C.; Liu, H.; Lu, C. CO_2 capture by carbide slag from chlor-alkali plant in calcination/carbonation cycles. *Int. J. Greenhouse Gas Control* **2012**, 9, 117-123.

(13) Sun, R.; Li, Y.; Liu, C.; Xie, X.; Lu, C. Utilization of lime mud from paper mill as CO_2 sorbent in calcium looping process. *Chem. Eng. J.* **2013**, 221, 124-132.

(14) Witoon, T. Characterization of calcium oxide derived from waste eggshell and its application as CO_2 sorbent. *Ceram. Int.* **2011**, 37, 3291-3298.

(15) Sabbas, T.; Polettini, A.; Pomi, R.; Astrup, T.; Hjelmar, O.; Mostbauer, P.; Cappai, G.; Magel, G.; Salhofer, S.; Speiser, C.; Heuss-Assbichler, S.; Klein, R.; Lechner, P. Management of municipal solid waste incineration residues. *Waste Manage.* **2003**, 23, 61-88.

(16) Foo, R.; Berger, R.; Heiszwolf, J.J. Reaction Kinetic Modeling of DSI for MATS Compliance. Power Plant Pollutant Control and Carbon Management "MEGA" Symposium (16-19 August 2016), Baltimore, MD (USA).

(17) Vehlow, J. Air pollution control systems in WtE units: an overview. *Waste Manage.* **2015**, 37, 58-74.

(18) Sun, J.; Bertos, M. F.; Simons, S.J.R. Kinetic study of accelerated carbonation of municipal solid waste incinerator air pollution control residues for sequestration of flue gas CO_2. *Energy Environ. Sci.* **2008**, 1, 370-377.

(19) Margallo, M.; Taddei, M.B.M.; Hernandez-Pellon, A.; Aldaco, R.; Irabien, A. Environmental sustainability assessment of the management of municipal solid waste incineration residues: a review of the current situation. *Clean Technol. Environ. Policy* **2015**, 17, 1333-1353.

(20) ISWA, Management of APC residues from WtE plants – an overview of management options and treatment methods, International Solid Waste Association, technical report, 2008. Available at: www.iswa.org/uploads/tx_iswaknowledgebase/Management_of_APC_residues_from_W-t-E_Plants_2008_01.pdf (last accessed: 10/01/2018)

(21) Wang, L.; Jin, Y.; Nie, Y. Investigation of accelerated and natural carbonation of MSWI fly ash with a high content of Ca. *J. Hazard. Mater.* **2010**, 174, 334-343.

(22) Quina, M.J.; Bordado, J.C.; Quinta-Ferreira, R.M. Treatment and use of air pollution control residues from MSW incineration: An overview. *Waste Manage.* **2008**, 28, 2097-2121.

(23) Van Gerven, T.; Geysen, D.; Stoffels, L.; Jaspers, M.; Wauters, G.; Vandecasteele, C. Management of incinerator residues in Flanders (Belgium) and in neighbouring countries. A comparison. *Waste Manage.* **2005**, 25, 75-87.

(24) Dal Pozzo, A.; Guglielmi, D.; Antonioni, G.; Tugnoli, A. Sustainability analysis of dry treatment technologies for acid gas removal in waste-to-energy plants. *J. Clean. Prod.* **2017**, 162, 1061-1074.

(25) Baciocchi, R.; Polettini, A.; Pomi, R.; Prigiobbe, V.; Von Zedwitz, V.N.; Steinfeld, A. CO_2 sequestration by direct gas-solid carbonation of air pollution control (APC) residues. *Energy Fuels* **2006**, 20, 1933-1940.

(26) Baciocchi, R.; Costa, G.; Di Bartolomeo, E.; Polettini, A.; Pomi, R. The effects of accelerated carbonation on CO_2 uptake and metal release from incineration APC residues. *Waste Manage.* **2009**, 29, 2994-3003.

(27) Arickx, S.; Van Gerven, T.; Vandecasteele, C. Accelerated carbonation for treatment of MSWI bottom ash. *J. Hazard. Mater.* **2006**, B137, 235-243.

(28) Ni, P.; Xiong, Z.; Tian, C.; Li, H.; Zhao, Y.; Zhang, J.; Zheng, C. Influence of carbonation under oxy-fuel combustion flue gas on the leachability of heavy metals in MSWI fly ash. *Waste Manage.* **2017**, 67, 171-180.

(29) Bobicki, E.R.; Liu, Q.; Xu, Z.; Zeng, H. Carbon capture and storage using alkaline industrial wastes. *Prog. Energy Combust. Sci.* **2012**, 38, 302-320.

(30) Pour, N.; Webley, P.A.; Cook, P.J. Potential for using municipal solid waste as a resource for bioenergy with carbon capture and storage (BECCS). *Int. J. Greenhouse Gas Control* **2018**, 68, 1-15.

(31) Antonioni, G.; Dal Pozzo, A.; Guglielmi, D.; Tugnoli, A.; Cozzani, V. Enhanced modelling of heterogeneous gas-solid reactions in acid gas removal dry processes. *Chem. Eng. Sci.* **2016**, 148, 140-154.

(32) De Greef, J.; Villani, K.; Goethals, J.; Van Belle, H.; Van Caneghem, J.; Vandecasteele, C. Optimising energy recovery and use of chemicals, resources and materials in modern waste-to-energy plants. *Waste Manage.* **2013**, 33, 2416–2424.

(33) Kim, K.-D.; Jeon, S.-M.; Hasolli, N.; Lee, K-S.; Lee, J.-R.; Han, J.-W.; Kim, H.-T.; Park, Y.-O. HCl removal characteristics of calcium hydroxide at the dry-type sorbent reaction accelerator using municipal waste incinerator flue gas at a real site. *Korean J. Chem. Eng.* **2017**, 34, 747-756.

(34) Broda, M.; Müller, C.R. Sol–gel-derived, CaO-based, ZrO_2-stabilized CO_2 sorbents. *Fuel* **2014**, 127, 94-100.

(35) Barontini, F.; Marsanich, K.; Cozzani, V. The use of TG-FTIR technique for the assessment of hydrogen bromide emissions in the combustion of BFRs. *J. Therm. Anal. Calorim.* **2004**, 78, 599-619.

(36) Biganzoli, L.; Racanella, G.; Rigamonti, L.; Marras, R.; Grosso, M. High temperature abatement of acid gases from waste incineration. Part I: Experimental tests in full scale plants. *Waste Manage.* **2015**, 36, 98-105.

(37) Dal Pozzo, A.; Guglielmi, D.; Antonioni, G.; Tugnoli, A.; Cozzani, V. Environmental assessment of combined acid gas emission control with alternative dry sorbent injection systems. *Chem. Eng. Trans.* **2017**, 57, 763-768.

(38) Goñi, S.; Guerrero, A. Accelerated carbonation of Friedel's salt in calcium aluminate cement paste. *Cem. Concr. Res.* **2003**, 33, 21-26.

(39) Pesce, G.L.; Fletcher, I.W.; Grant, J.; Molinari, M.; Parker, S.C.; Ball, R.J. Carbonation of Hydrous Materials at the Molecular Level: A Time of Flight-Secondary Ion Mass Spectrometry, Raman and Density Functional Theory Study. *Cryst. Growth Des.* **2017**, 17, 1036-1044.

(40) Fonseca, A.M.; Orfao, J.J.; Salcedo, R.L. Dry Scrubbing of Gaseous HCl with Solid Lime in a Cyclone Reactor at Low Temperatures. *Ind. Eng. Chem. Res.* **2001**, 40, 304-313.

(41) Garea, A.; Marqués, J.A.; Irabien, A.; Kavouras, A.; Krammer, G. Sorbent behavior in urban waste incineration: acid gas removal and thermogravimetric characterization, *Thermochim. Acta* **2003**, 397, 227-236.

(42) Dal Pozzo, A.; Moricone, R.; Antonioni, G.; Tugnoli, A.; Cozzani, V. Hydrogen Chloride Removal from Flue Gas by Low-Temperature Reaction with Calcium Hydroxide. *Energy Fuels* **2018**, 32 (1), 747-756.

(43) Prigiobbe, V.; Polettini, A.; Baciocchi, R. Gas–solid carbonation kinetics of Air Pollution Control residues for CO_2 storage. *Chem. Eng. J.* **2009**, 148, 270-278.

(44) Stanmore, B.R.; Gilot, P. Review—calcination and carbonation of limestone during thermal cycling for CO_2 sequestration. *Fuel Process. Technol.* **2005**, 86, 1707-1743.

(45) Bogush, A.; Stegemann, J.A.; Wood, I.; Roy, A. Element composition and mineralogical characterisation of air pollution control residue from UK energy-from-waste facilities. *Waste Manage.* **2015**, 36, 119-129.

(46) Geysen, D.; Vandecasteele, C.; Jaspers, M.; Brouwers, E.; Wauters, G. Effect of improving flue gas cleaning on characteristics and immobilization of APC residues from MSW incineration. *J. Hazard. Mater.* **2006**, B128, 27-38.

(47) Baciocchi, R.; Costa, G.; Gavasci, R.; Lombardi, L.; Zingaretti, D. Regeneration of a spent alkaline solution from a biogas upgrading unit by carbonation of APC residues. *Chem. Eng. J.* **2012**, 179, 63-71.

(48) Yan, Z.; Wang, Z.; Liu, H..; Tu, Y.; Yang, W.; Zeng, H.; Qiu, J. Decomposition and solid reactions of calcium sulfate doped with SiO_2, Fe_2O_3 and Al_2O_3. *J. Anal. Appl. Pyrolysis* **2015**, 113, 491-498.

(49) Al-Shawabkeh, A.; Lin, S.-Y.; Matsuda, H.; Hasatani, M. Formation behavior of $CaSO_3$ during high-temperature desulfurization with Ca-based sorbents. *J. Chem. Eng. Jpn.* **1995**, 28, 689-696.

(50) Dennis, J.S.; Pacciani, R. The rate and extent of uptake of CO_2 by a synthetic, CaO-containing sorbent. *Chem. Eng. Sci.* **2009**, 64, 2147-2157.

(51) Tian, S.; Jiang, J. Sequestration of Flue Gas CO_2 by Direct Gas-Solid Carbonation of Air Pollution Control System Residues. *Environ. Sci. Technol.* **2012**, 46, 13545-13551.

(52) Broda, M.; Kierzkowska, A.M.; Müller, C.R. Development of Highly Effective CaO-based, MgO-stabilized CO_2 Sorbents via a Scalable "One-Pot" Recrystallization Technique. *Adv. Funct. Mater.* **2014**, 24, 5753–5761.

(53) Alvarez, D.; Abanades, J.C. Determination of the Critical Product Layer Thickness in the Reaction of CaO with CO_2. *Ind. Eng. Chem. Res.* **2005**, 44, 5608-5615.

(54) Gonzalez, B.; Blamey, J.; McBride-Wright, M.; Carter, N.; Dugwell, D.; Fennell, P.; Abanades, J.C. Calcium looping for CO_2 capture: sorbent enhancement through doping. *Energy Procedia* **2011**, 4, 402-409.

(55) Al-Jeboori, M.J.; Fennell, P.S.; Nguyen, M.; Feng, K. Effects of Different Dopants and Doping Procedures on the Reactivity of CaO-based Sorbents for CO_2 Capture. *Energy Fuels* **2012**, 26, 6584-6594.

(56) Manovic, V.; Fennell, P.S.; Al-Jeboori, M.J.; Anthony, E.J. Steam-Enhanced Calcium Looping Cycles with Calcium Aluminate Pellets Doped with Bromides. *Ind. Eng. Chem. Res.* **2013**, 52, 7677-7683.

(57) Li, Y.; Ma, X.; Wang, W.; Chi, C.; Shi, J.; Duan, L. Enhanced CO_2 capture capacity of limestone by discontinuous addition of hydrogen chloride in carbonation at calcium looping conditions. *Chem. Eng. J.* **2017**, 316, 438-448.

(58) Li, Y.; Wang, W.; Cheng, X.; Su, M.; Ma, X.; Xie, X. Simultaneous CO_2/HCl removal using carbide slag in repetitive adsorption/desorption cycles. *Fuel* **2015**, 142, 21-27.

(59) Chin, T.; Yan, R.; Liang, D.T.; Tay, J.H. Hydrated lime reaction with HCl under simulated flue gas conditions. *Ind. Eng. Chem. Res.* **2005**, 44, 3742-3748.

(60) Wang, W.; Li, Y.; Xie, X.; Sun, R. Effect of the presence of HCl on cyclic CO_2 capture of calcium-based sorbent in calcium looping process. *Appl. Energy* **2014**, 125, 246-253.

(61) Freidina, E.B.; Fray, D.J. Phase diagram of the system $CaCl_2$-$CaCO_3$. *Thermochim. Acta* **2000**, 351, 107-108.

(62) Abanades, J.C.; Alvarez, D. Conversion Limits in the Reaction of CO_2 with Lime. *Energy Fuels* **2003**, 17, 308-315.

(63) Valverde, J.M.; Sanchez-Jimenez, P.E.; Perez-Maqueda, L.A. Calcium-looping for post-combustion CO_2 capture. On the adverse effect of sorbent regeneration under CO_2. *Appl. Energy* **2014**, 126, 161-171.

(64) Manovic, V.; Charland, J.-P.; Blamey, J.; Fennell, P.S.; Lu, D.Y.; Anthony, E.J. Influence of calcination conditions on carrying capacity of CaO-based sorbent in CO_2 looping cycles. *Fuel* **2009**, 88, 1893-1900.

(65) Lindberg, A.; Molin, C.; Hupa, M. Thermal treatment of solid residues from WtE units: A review. *Waste Manage.* **2015**, 37, 82-94.

(66) Dean, C.C.; Blamey, J.; Florin, N.H.; Al-Jeboori, M.J.; Fennell, P.S. The calcium looping cycle for CO_2 capture from power generation, cement manufacture and hydrogen production. *Chem. Eng. Res. Des.* **2011**, 89, 836-855.

(67) Helbig, M.; Hilz, J.; Haaf, M.; Daikeler, A.; Ströhle, J.; Epple, B. Long-term carbonate looping testing in a 1 MW_{th} pilot plant with hard coal and lignite. 13th International Conference on Greenhouse Gas Control Technologies (GHTG-13), November 2016, Lausanne (Switzerland).

(68) Diego, M.E.; Arias, B.; Abanades, J.C. Evolution of the CO_2 carrying capacity of CaO particles in a large calcium looping pilot plant. *Int. J. Greenhouse Gas Control* **2017**, 62, 69-75.

(69) Dal Pozzo, A.; Antonioni, G.; Guglielmi, D.; Stramigioli, C.; Cozzani, V. Comparison of alternative flue gas dry treatment technologies in waste-to-energy processes. *Waste Manage.* **2016**, 51, 81-90.